Journal of Electronics and Electrical Engineering
https://ojs.wiserpub.com/index.php/JEEE

Research Article

Analysis on Performance of HTS DC Cables with Counter-Flow Cooling Mode

Jian Cheng[1], Zhiyi Luo[1], Fengyin Zhang[1], Weili Zhao[1], Quan Zhang[1], Bangzhu Wang[2], Ziqing Meng[3*]

[1] Shenzhen Power Supply Bureau Co., Ltd., China Southern Power Grid, Shenzhen, 518000, China
[2] School of Electrical Engineering, Beijing Jiaotong University, Beijing, 100044, China
[3] School of Electrical Engineering, North China Electric Power University, Beijing, 102206, China
E-mail: 13389581662@163.com

Received: 29 March 2025; **Revised:** 12 May 2025; **Accepted:** 28 May 2025

Abstract: With the increase in power demand, the transmission distance of the high-temperature superconducting (HTS) direct current (DC) cable is required to be longer. However, the impact of temperature changes caused by the increase in cable length on cable performance is rarely considered. This paper focuses on the effects of two different cooling arrangements on the performance of km-class HTS DC cables. The analysis reveals that the cooling method significantly influences the temperature distribution along the cable, which in turn affects the critical current and effectiveness of the cable. The findings underscore the importance of optimizing cooling strategies to enhance the reliability and efficiency of km-class HTS DC cables with ripple current in practical applications.

Keywords: HTS DC cable, cooling arrangement, critical current, ripple current

1. Introduction

High-temperature superconducting (HTS) direct current (DC) cables represent a significant advancement in electrical power transmission technology, offering reduced energy losses and improved efficiency compared to conventional copper and aluminum cables [1]. These cables are particularly beneficial for long-distance power transmission applications, where minimizing resistance losses is crucial for maximizing transmission efficiency [2], [3]. A 2 km long superconducting DC cable, supported by the New Energy and Industrial Technology Development Organization, was scheduled to be introduced in 2021 [4]. With the increase in power demand, the transmission distance of the HTS DC cable is required to be longer.

However, the efficiency of these cables is highly dependent on the cooling arrangements, particularly in long cable applications, where thermal management becomes crucial [5]. As the critical current of superconducting tapes is a temperature dependent quantity, an increase in cable length is inevitably accompanied by a change in temperature, which affects the performance of the cable. Besides, ripple currents, primarily caused by imperfections in rectifier systems, pose significant challenges leading to dynamic resistance and uneven current distributions within the superconducting tapes.

Currently, numerous studies have employed numerical and analytical models across various technologies and implementations to estimate cable current distribution and AC losses [6], [7]. Especially for long HTS DC cables, [8] has proposed that the cable experiencing ripple currents will exhibit dynamic resistance R_{dy}, contact resistance R_c, and flux flow resistance R_{ff} in the circuit, which should be considered simultaneously in design.

DOI: https://doi.org/10.37256/jeee.4120256868

Upon on prior work, this paper has further investigated the general cooling arrangements to achieve high performance in km-class HTS DC cables operating under ripple current conditions.

On the whole, the main research content of this paper is as follows:

1) The variation of R_{dy} with ripple current fluctuation was plotted, then the data of DC distribution and current margin affected by ripple current in each layer were also obtained.

2) The temperature variation is taken into account when the cable transmission distance is relatively long, and two common cooling modes are used to analyze the temperature gradient varying with cable length.

3) As for R_{ff}, its contribution to loss is the most concerned, but previous references only consider the influence of R_c, we thoroughly take the influence of three types of resistances (R_{ff}, R_c, R_{dy}) into account, and the loss distribution due to temperature gradient along long-length was systematically analyzed and calculated.

Our analysis reveals that non-uniform current distributions induced by three types of resistances can precipitate thermal instability in HTS DC cables, potentially leading to catastrophic failure. Furthermore, R_{ff} losses exhibit non-constant behavior under operational conditions, with their cumulative impact posing critical stability risks in long-distance transmission scenarios. The findings will enhance the design and reliability of HTS cable systems for practical applications.

2. Cooling arrangements

Generally, in order to cool the HTS tape in long cables, a counter-flow cooling arrangement, or a parallel-flow arrangement is commonly utilized [9]. This paper primarily examines the counter-flow cooling arrangement, as it optimizes space and reduces thermal load by enabling the coolant to return to its source within the cable itself, rather than necessitating a separate return pipe. It is assumed that the mass flow of the liquid nitrogen (LN_2), is the same in parallel-flow and counter-flow directions, and the mass flow rate denoted as M = 0.25 kg/s [10]. Two widely adopted configurations for the cooling of long cables are described in the following sections.

2.1 *Counter-flow cooling arrangement with single refrigeration station*

Figure 1a illustrates the flowchart of a two-dimensional (2D) analytical model featuring a single refrigeration station within counter-flow cooling system. A refrigeration unit is positioned at the liquid nitrogen inlet, where the temperature of the nitrogen is designated as the initial temperature T_0, typically set to 70 K. Notably, the temperatures of the inner and outer channels at the end of the cable are equal, represented mathematically as $T_i(L) = T_o(L)$. However, this arrangement could potentially lead to thermal short-circuiting if the thermal conductivity between the liquid nitrogen (LN_2) in-flow and counter-flow is not sufficiently low.

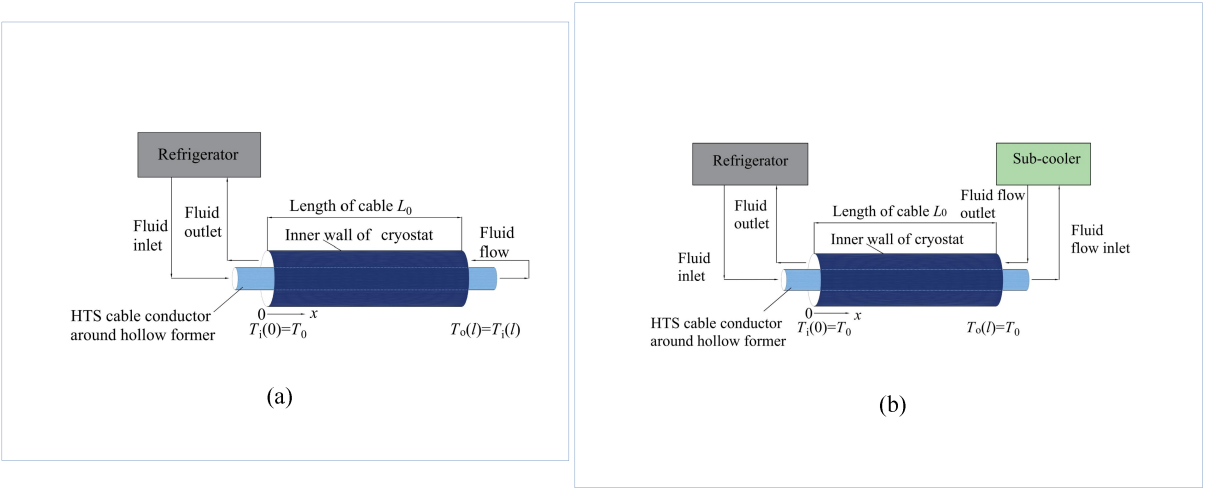

Figure 1. Counter-Flow cooling arrangement (a) single refrigeration station (b) with sub-cooled station

2.2 *Counter-flow cooling arrangement with a sub-cooled station*

In order to effectively cool the long HTS cable using the counter-flow mode and ensure normal operation, an additional counter-flow cooling system with a sub-cooled station is installed at the opposite end of the cable, as illustrated in Figure 1b. Since the secondary refrigeration station is used, the temperature of liquid nitrogen at the inlet of the internal and outer channels is the same, which is the initial temperature T_0 of the refrigeration station, that is, $T_i(0) = T_o(L) = T_0$.

Table 1. Thermo-physical characteristics of LN_2 at 77 K and 0.1 MP

Items	Value
Inlet temperature T_0/K	70
The heat from AC loss P/(W/m)	1.39
Heat leakage from exterior P_0/(W/m)	0.85
Thermal conductivity of dielectric insulation k/(W/m/K)	0.05
Capacity C_p/(J/m^3/K)	2,051
Dynamic viscosity μ/(Pa·s)	216×10^{-6}
Density ρ/(kg/m^3)	837
Thermal conductivity of LN_2 k_{LN_2}/(W/m/K)	0.15

Nevertheless, no matter which cooling mode is adopted, due to the flow friction loss of LN_2, heat leakage from exterior P_0 and AC loss P, when the LN_2 flows in the cooling channel, there is a difference in temperature between the inner and outer LN_2 channels along long lengths. Preliminary estimates of P and P_0 are set at 1.39 W/m and 0.85 W/m, respectively [9].

The relationship between temperature T (K) and cable length x (m) under these two cooling modes can be calculated by (1)-(4) and the thermo-physical characteristics of LN_2 at 77 K and 0.1 MP are listed in Table 1 [11]. Equations (1) and (2) apply to single refrigerator mode, while (3), and (4) are the results obtained by using two refrigerator modes.

$$T_i(x) = -\frac{\pi K(P+P_0)}{C_p{}^2M^2}x^2 + \frac{1}{C_pM}\left[\frac{2\pi K(P+P_0)}{C_pM}L + \frac{P}{2}\right]x + T_0 \quad (1)$$

$$T_o(x) = -\frac{\pi K(P+P_0)}{{C_p}^2 M^2}x^2 + \frac{1}{C_p M}\left[\frac{2\pi K(P+P_0)}{C_p M}L - \frac{P+2P_0}{2}\right]x + T_0 + \frac{(P+P_0)}{C_p M}L \tag{2}$$

$$T_i(x) = -\frac{\pi K(P+P_0)}{{C_p}^2 M^2}x^2 + \frac{2\pi K}{C_p M}\frac{\frac{(P+2P_0)L}{2} + \frac{\pi K}{C_p M}(P+P_0)L^2}{2\pi KL + C_p M}x + \frac{P}{2C_p M}x + T_0 \tag{3}$$

$$T_o(x) = -\frac{\pi K(P+P_0)}{{C_p}^2 M^2}x^2 + \left(\frac{2\pi K}{C_p M}\frac{\frac{(P+2P_0)L}{2} + \frac{\pi K}{C_p M}(P+P_0)L^2}{2\pi KL + C_p M} - \frac{P+2P_0}{2C_p M}\right)x + \frac{\frac{(P+2P_0)L}{2} + \frac{\pi K}{C_p M}(P+P_0)L^2}{2\pi KL + C_p M} + T_0 \tag{4}$$

where T_i(l) and T_o(l) stand for the inner and outer channels' temperatures, respectively. K is the assumed linear conductance, can be calculated in [11], and C_p represents the capacity of LN_2.

According to the structure of the four-layer HTS DC cable in [8], the inner two layers of tape are set to the LN_2 temperature of the inner channel, while the rest two layers are turned to the LN_2 temperature of the outer channel.

3. Performance of km-class HTS DC cable with ripple current

3.1 *Analysis and calculation of the current distributions*

Current distribution is an important indicator for evaluating cable performance, and the calculation method is detailed in [12]. In an ideal situation, HTS cables have zero resistance, and the current distribution should be uniform, which is also more conducive to the stable operation of the cable. However, in practical situations, issues with the rectifier lead to the inevitable accumulation of AC ripple current on the DC current flowing through the superconducting tape. Once the amplitude of the AC magnetic field generated by the ripple current exceeds its threshold, dynamic resistance (R_{dy}) will occur. It is well established that R_{dy} largely depends on the external AC magnetic field, rather than the transmission distance. Taking the design of the conceptual cable in [8] as an example, the specific information about the cable is listed in Table 2, the winding radius of each layer of the cable is calculated according to the design of the uniform current method [12]. With a fixed transmission distance of 1 km and a predetermined temperature, the distribution of R_{dy} with different ripple coefficients on each layer can be calculated by Equations (5) and (6). As described in Figure 2, it is shown that a rise in ripple current results in a rising R_{dy} value in each layer of the cable, except in the first layer, where R_{dy} are zero for all ripple coefficients, since AC magnetic fields have a smaller amplitude than penetration fields.

Table 2. Main parameters of model HTS cable [8]

Items	Value
The thickness of the HTS tape a/mm	1
The width of the HTS tape w/mm	4
Number of layers of cable	4
1st layer radius r_{1i}/mm	8.18
2nd layer radius r_{2i}/mm	8.4
3rd layer radius r_{3i}/mm	8.63
4th layer radius r_{4i}/mm	8.85
Winding direction of each layer	−1, −1, 1, 1
No. tapes of each layer	11, 11, 12, 11
Rated current I/kA	5
Length L_0/km	1
n	26

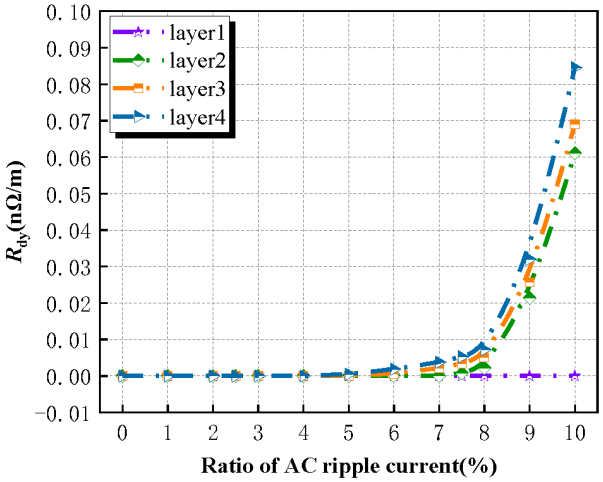

Figure 2. Distribution of dynamic resistance among layers with different ripple coefficients at the fixed power transmission distance L = 1 km

$$R_{dy}(T) = \frac{2af}{I_c(B,T)}(B_m - B_{th}) \tag{5}$$

where a denotes the thickness of the HTS tape, while f and B_m represent the frequency and amplitude of the applied AC magnetic field, respectively. The threshold magnetic field B_{th} is defined according to:

$$B_{th} = \mu_0 I_c/(2w)\left(1 - \frac{I_{dc}}{I_c(B,T)}\right) \tag{6}$$

where μ_0 is the magnetic permeability of vacuum, w corresponds to the width of the HTS tape, and I_{dc} is the magnitude of the DC transport current.

As for $I_c(B, T)$, which represents the tape's critical current and is dependent on temperature T and magnetic field B, which can be calculated by the following equation:

$$I_c(B,T) = I_c(B)(\frac{92-T}{92-20})^a \tag{7}$$

where $I_c(B)$ is generally expressed by well-known like-Kim model, the second term of right is dependent temperature, B is vector including magnitude and orientation. According to our experiment and fitting data [7], power index a is 1.15-1.25 in temperature range of 65 K-77 K, and 1.8-2.0 in temperature range of 20 K-40 K, which depends on different manufacturers and technologies.

In addition to R_{dy}, contact resistance R_c and flux flow resistance R_{ff} jointly affect the current distribution of superconducting cables. As well, R_{ff} is a DC resistance and can be calculated by equations in [7], the value of contact resistance is constant, generally 0.1 $\mu\Omega$, both are independent of ripple current. Figure 3 shows the DC distribution among layers of the conceptual cable, with ripple coefficients of 5%, 7.5%, and 10% as examples. Although the design method of uniform ripple current is employed, it is evident that the resistances in the circuit have a significant impact on the DC distribution.

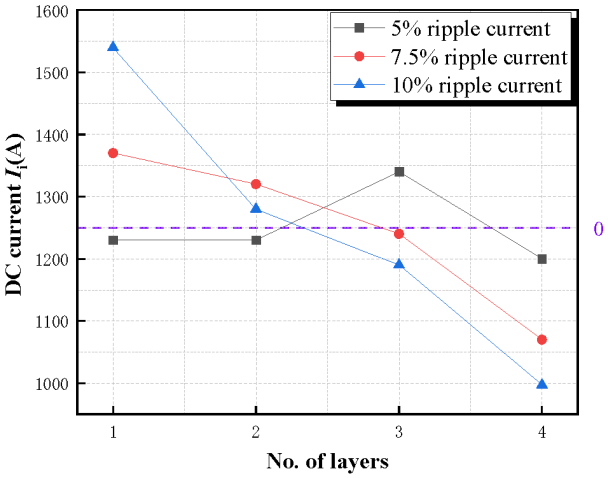

Figure 3. DC distribution among layers with different ripple coefficients at the fixed power transmission distance L = 1 km

For the 5 kA 4-layer HTS DC cable in [8], if the ripple current coefficient is 5%, R_{dy} can be ignored, as shown in Figure 2, the current distribution is relatively uniform (the high current in the third layer because the number of tapes is more than other layers and the R_{ff} as well as R_c also play a role). However, with the increase in ripple current, R_{dy} becomes the main cause of uneven current distribution, as Figure 3 illustrates, the current from the innermost layer to the outermost layer of the cable shows a downward trend when the ripple current coefficient reaches 10%. Since the current distribution between the tapes of HTS cables is highly non-uniform, it needs to be taken into consideration to ensure maximum reliability and optimal performance [13].

As R_{ff} appears once the operating current I_{op} approaches its critical current I_c, and the worst result is that the superconducting tape quenches. With the consideration of the safety margin, the normalized currents among 4 layers of the cable with 5%, 7.5%, and 10% ripple coefficients are calculated as shown in Figure 4, where I_{opi} represents the sum of DC I_i and AC I_{mi} of the ith-layer. Evidently, at different ripple current coefficients, the normalized current shows different rules in each layer. If the ripple current coefficient is 5%, the normalized current increases layer by layer, but decreases gradually at 10% and appears relatively uniform at 7.5%. The normalized current at each layer with huge differences needs to be paid attention to, as the current margin of the whole cable should be determined by the lowest critical current. Consequently, the outermost layer of the cable is most likely to quench when the ripple current coefficient is 5% as its operating current I_{op} is nearest the critical current I_c. But the result is the opposite if the coefficient reaches 10%, the figure shows that the innermost layer is easier to quench.

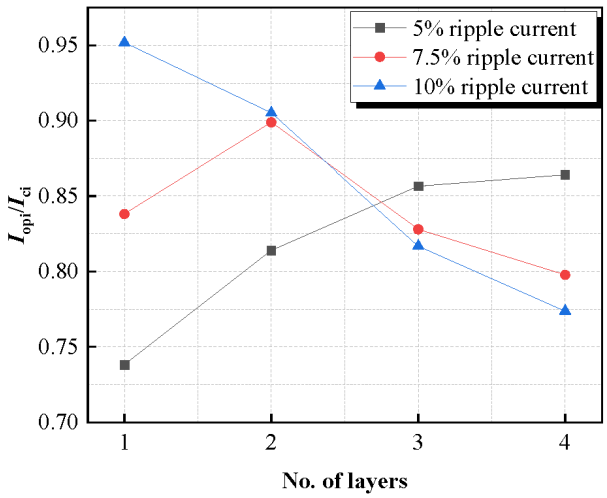

Figure 4. Normalized total current distributions among layers with different ripple coefficients at the fixed power transmission distance L = 1 km

However, for long cables, it is insufficient to consider only the ripple current; the impact of cable length must also be taken into account. Given that the temperature along the cable varies, we take 100 m as a research unit, then the temperature at the LN_2 inlet along the inner channel T_i and the outer channel T_o can be obtained.

In the mode of only a single refrigerator, as displayed in Figure 5a, T_i gradually increases along the length and reaches about 76 K at the end of the cable. However, T_o shows a different appearance, and the maximum value is close to 77 K at the position of 600 m in the cable. The critical current I_{ci} is a temperature dependent parameter, and the normalized current of a long cable will vary accordingly, ultimately approaching 76%, slightly higher than the rated parameter of 64.6% in [8].

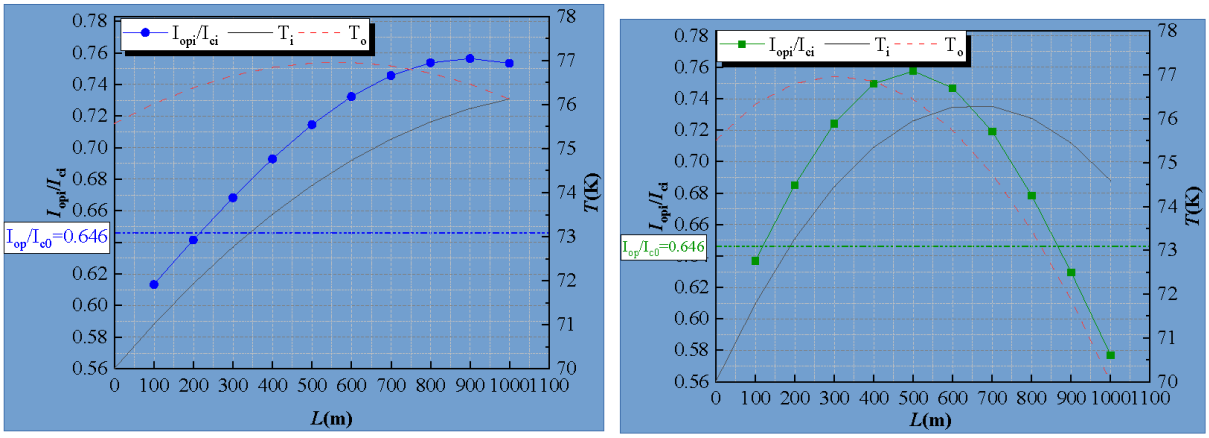

Figure 5. Variation of normalized operating current (left) and temperature (right) with the increasing transmission distance L (a) single refrigeration station (b) with sub-cooled stations

In Figure 5b, due to the existence of the second refrigerator, the temperature at the end of the cable is not as high as if there is only one refrigerator though its maximum temperature also approaches 77 K in the outer channel.

Affected by such internal and external channel temperatures, the normalized current rises first and then decreases gradually, and there will be a minimum value at the end of the line which is about 57.9%, which can be attributed to the second refrigerator. However, in this way, the temperature in the middle of the cable, about 500 m away, will be very high, and its normalized current is almost 76%.

In a word, no matter which cooling mode is adopted, the temperature rise of superconducting tape is inevitable, and that is the reason why we should deliberate the temperature factor for the safe operation of long superconducting cables.

3.2 *Analysis and calculation of the cable loss*

Not only safety but also economy is essential in the design process of the HTS DC cable. Considering the length factor, the total AC losses consist of terminal contact resistance loss P_j, the hysteresis loss P_h, as well as the loss caused by the flux-flow resistance P_{ff}, can be calculated as:

$$P_{total} = \sum_{i=1}^{n} P_{ji} + P_{hi} + P_{ffi} \tag{8}$$

where n represents the number of layers in the HTS DC cable.

HTS DC cables generally have small ripple currents compared to DC components, so we use an example with a 5% ripple coefficient, then the loss per 100 m of different components can be calculated [8], as illustrated in Figure 6.

In both cooling modes, it can be seen that under the uniform current design principle, P_j appears constant compared with other losses which vary with the power transmission distance. And P_h is relatively inconspicuous as it is mainly related to the AC magnetic field.

Along the cable length, P_{ff} increases first and then decreases, and there is a maximum value at the position of 600 m with a single refrigeration station, which is approximately equal to 1.51 mW/m. Besides, when the second refrigerator is used, the P_{ff} only shows high in the first half of the cable and reaches its maximum value at the position of 300 m and almost 1.59 mW/m.

To prevent the influence of P_{ff}, it is necessary to control the temperature of both the inner and outer channels at a very low level. However, with the existing cooling methods and manufacturing costs of HTS DC cables, it is difficult due to the inevitable flow friction loss of LN_2, heat leakage from the exterior and AC loss in practice [14]. Therefore, the issue with large loss caused by temperature gradient along the length of km-class HTS DC cable is worthy of our consideration. Accurately simulation and experiments are of great significance for the future development of HTS DC cables towards practical longer distances.

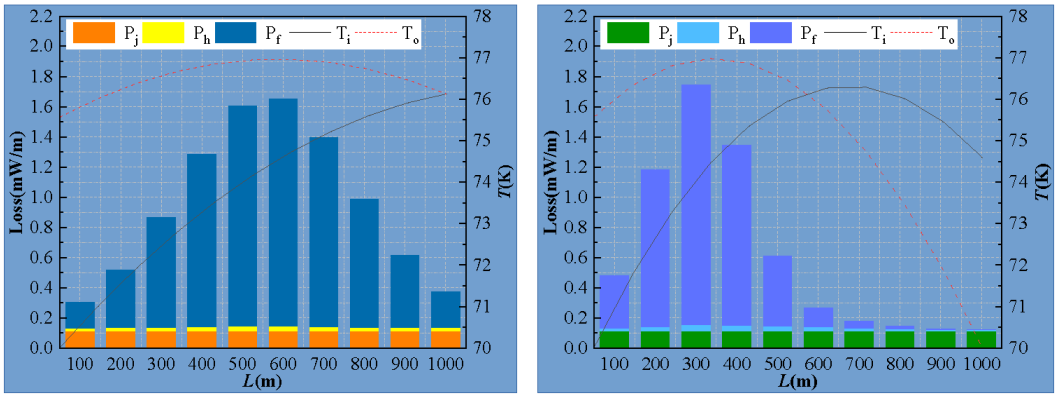

Figure 6. Different composition of AC losses and temperature with the increasing transmission distance L. (a) single refrigeration station (b) with sub-cooled station

4. Conclusions

A systematized analysis of DC distribution and AC loss is presented for km-class HTS DC cables accompanied by ripple current following the typical uniform current design approach. The results show that the excessive ripple current contributes greatly to creating R_{dy} and then the current imbalance of the HTS DC cable, which is detrimental to the long-term stable operation of the cable and even probably causes the cable to quench. As a further finding, the analysis of km-class HTS DC cables cooled by two common counter-flow arrangements indicates that the fluctuations of temperature and I_c along the length direction can result in the cable's capacity being reduced and performance degraded. Especially, the R_{ff}, which is most affected by temperature, has an exponential relationship with temperature according to our calculation results.

Funding

This work was supported by the China Southern Power Grid Major Science and Technology Program under Grant 090000KK52222197.

Conflict of interest

There is no conflict of interest for this study.

References

[1] D. Zhang, S. Dai, F. Zhang, T. Huang, Y. Wang, Y. Lin, Y. Teng, G. Zhang, L. Xiao, and L. Lin, "Design research on the conductor of 10 kA class HTS DC power cable," *Cryogenics*, vol. 52, no. 12, pp. 725-729, 2012.

[2] B. Yang, J. Kang, S. Lee, C. Choi, and Y. Moon, "Qualification test of an 80 kV 500 MW HTS DC cable for applying into real grid," *IEEE Transactions on Applied Superconductivity*, vol. 25, no. 3, p. 5402705, Feb. 2015.

[3] V. E. Sytnikov, S. E. Bemert, Yu. V. Ivanov, S. I. Kopylov, I. V. Krivetskiy, D. S. Rimorov, M. S. Romashov, Yu. G. Shakaryan, R. N. Berdnikov, Yu. A. Dementyev, Yu. A. Goryushkin, and D. G. Timofeev, "HTS DC cable line project: On-going activities in Russia," *IEEE Transactions on Applied Superconductivity*, vol. 23, no. 3, p. 5401904, Feb. 2013.

[4] M. Tomita, K. Suzuki, Y. Fukumoto, A. Ishihara, T. Akasaka, and Y. Kobayashi, "Energy-saving railway systems based on superconducting power transmission," *Energy*, vol. 122, pp. 579-587, Mar. 2017.

[5] Y. V. Ivanov, H. Watanabe, N. Chikumoto, M. Hamabe, H. Takano, J. Sun, and S. Yamaguchi, "Thermosiphon effect during cooling test of a 200 m DC HTS cable facility," *IEEE Transactions on Applied Superconductivity*, vol. 26, no. 3, p. 5401204, Jan. 2016.

[6] F. Grilli, "Numerical modeling of high temperature superconducting tapes and cables," Ph.D. dissertation, EPFL, Lausanne, Switzerland, 2004. [Online]. Available: https://infoscience.epfl.ch/record/33710. [Accessed May 28, 2025]

[7] Y. S. Wang, Z. Q. Meng, W. Liu, J. Wang, H. Zhang, H. Zhang, and W. Pi, "Influence of dynamic resistance on current distribution of HTS DC cable conductor for feeder lines and large-scale magnet," *IEEE Transactions on Applied Superconductivity*, vol. 32, no. 6, p. 4801906, Mar. 2022.

[8] Z. Q. Meng, Y. S. Wang, J. H. Cheng, and W. Pi, "Influence of flux-flow and terminal contacting as well as dynamic resistances due to ripple current on performance of the km-class HTS DC cable," *IEEE Transactions on Applied Superconductivity*, vol. 34, no. 8, p. 5403505, Sep. 2024.

[9] Y. S. Wang, *Fundamental Elements of Applied Superconductivity in Electrical Engineering*. Singapore: John Wiley & Sons Singapore Pte. Ltd., 2013, pp. 430-435.

[10] C. Humpert, "Long distance transmission systems for the future electricity supply-Analysis of possibilities and restrictions," *Energy*, vol. 48, no. 1, pp. 278-283, Dec. 2012.

[11] S. Fuchino, M. Furuse, and N. Higuchi, "Longitudinal temperature distribution in superconducting power cables with counter-flow cooling," *IEEE Transactions on Applied Superconductivity*, vol. 12, no. 1, pp. 1339-1342, Aug. 2002.
[12] H. Zhang, Y. Wang, C. Kan, Y. Fu, and J. Xue, "Effects of HTS tape arrangements on AC loss in self-shielding DC HTS cable with AC ripple current," *IEEE Transactions on Applied Superconductivity*, vol. 27, no. 4, p. 4800605, Dec. 2016.
[13] J. H. Kim, C. H. Kim, V. Pothavajhala, and S. V. Pamidi, "Current sharing and redistribution in superconducting DC cable," *IEEE Transactions on Applied Superconductivity*, vol. 23, no. 3, p. 4801304, Feb. 2013.
[14] S. Fuchino, M. Furuse, and N. Higuchi, "Longitudinal temperature distribution in superconducting power cables with counter-flow cooling," *IEEE Transactions on Applied Superconductivity*, vol. 12, no. 1, pp. 1339-1342, Aug. 2002.